JMEPEG (2011) 20:819–823
DOI: 10.1007/s11665-011-9874-7

1059-9495/$19.00

Effect of Manufacturing Process on the Biocompatibility and Mechanical Properties of Ti-30Ta Alloy

P. Gill, N. Munroe, C. Pulletikurthi, S. Pandya, and W. Haider

(Submitted June 18, 2010; in revised form January 28, 2011)

Ti alloys have been widely used in the aerospace, chemical, and biomedical industries for their high strength/weight ratio and corrosion resistance. However, Nitinol's usage in the latter industry has been fraught with concerns of allergic and toxic effects of Ni released from implants. Recently, much attention has been placed on the development of Ni-free Ti-Ta alloys, which are considered prime candidates for applications such as metal-on-metal spinal disk replacements, orthopedic implants, cardiovascular stents, dental posts, and guide wires. In this research, the biocompatibility of Ti-30Ta alloys manufactured by powder metallurgy (PM) and arc melting (ARC) were investigated. The corrosion resistance of each alloy was determined in accordance with ASTM F 2129-08 in phosphate buffered saline (PBS) and PBS with amino acids at 37 °C. The concentration of metal ions released during corrosion was measured by Inductively Coupled Plasma Mass Spectroscopy (ICP-MS). Scanning Electron Microscopy (SEM) was used to assess the morphology of the alloys before and after corrosion. Vicker's hardness tests were performed to compare the hardness and tensile strength of the alloys. Human osteoblast cells were successfully grown on the surface of both alloys.

Keywords biocompatibility, corrosion, osteointegration

1. Introduction

There has been a steep increase in the relative proportion of senior citizens in society and so has the demand for replacement of failed tissue and organs with biomaterials and artificial devices (Ref 1). For example, an 8% annual growth is anticipated in the orthopedic industry from $6 billion in 2007 to $13 billion by 2017 (Ref 2). To meet this demand, a wide variety of biomaterials comprising polymers, ceramics, and metals are being developed. However, the biocompatibility of many of these materials has not been fully investigated. Class I materials (Ref 3) have no direct contact with bodily tissues, whereas Class II materials are in contact with tissues intermittently. Nevertheless, Class III materials that are constantly in contact with tissue are prone to unwanted ion leaching (Ref 3) and can be categorized into three types; bioinert, bioactive, and biodegradable. In this investigation, the biocompatibility and mechanical properties of the bioinert Ti-30Ta alloy was studied. The two highly passivating elements of this alloy form an extremely stable and protective oxide surface layer, which is responsible for its high resistance to corrosion and good biocompatibility (Ref 4-6).

This article is an invited paper selected from presentations at Shape Memory and Superelastic Technologies 2010, held May 16-20, 2010, in Pacific Grove, California, and has been expanded from the original presentation.

P. Gill, N. Munroe, C. Pulletikurthi, and **S. Pandya**, Mechanical and Materials Engineering Department, Florida International University, Miami, FL; and **W. Haider**, Materials Science and Engineering, Penn State University, University Park, PA. Contact e-mail: pgill001@fiu.edu.

2. Experimental Procedure

2.1 Materials

Two types of Ti-30Ta wt.% alloys were used in this investigation; one manufactured by PM (Dynamet Technology Inc.) and the other by ARC melting (National Institute of Standards and Technology (NIST)). The alloys were cut into disks (2.032 mm thick and 1.052 cm OD) using a linear precision saw (ISOMET 4000). The PBS and amino acids were purchased from Sigma Aldrich and Acros Organics, respectively.

2.2 Methodology

Samples were mechanically polished and cleaned ultrasonically in acetone, ethyl alcohol, and distilled water for 5 min each, prior to conducting corrosion and osteointegration studies. The corrosion resistance of the alloys was assessed by cyclic potentiodynamic polarization corrosion tests in accordance with ASTM F 2129-08 (Ref 7) in PBS, 0.01 mg/mL bovine serum albumin (BSA) in PBS and 0.102 mg/mL glutamine (G), 0.015 mg/mL histidine (H), and 0.01 mg/mL tryptophan (T) in PBS at 37 °C. The ASTM F 2129-08 standard is used to determine the corrosion resistance of implants. A typical three-electrode (working, counter, and reference) corrosion cell interphased with a potentiostat (GAMRY®) was used, in which the implant material (working electrode) is placed in an appropriate deaerated simulated physiological solution (PBS). The rest potential (E_r) is recorded for 1 h or until E_r stabilizes to a rate of change less than 3 mV/min (Ref 7). The potential between the working electrode and the reference electrode (saturated calomel electrode, SCE) is increased from E_r in the positive direction. The current flowing between the working

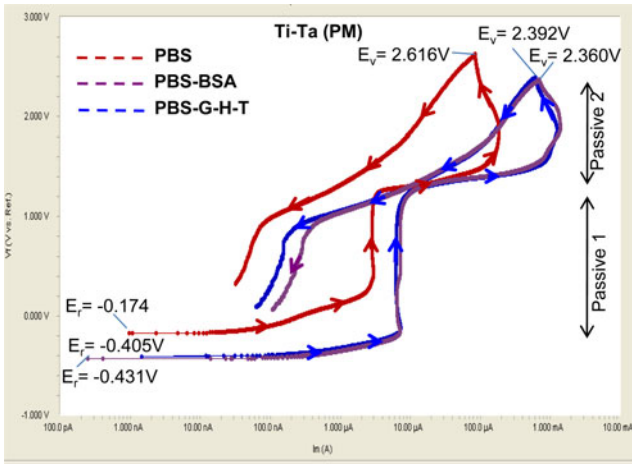

Fig. 1 Cyclic polarization curves for Ti-30Ta (PM) alloy (anti clockwise loop, no hysteresis) in PBS, PBS-BSA, and PBS-G-H-T

electrode and the counter electrode (carbon) is measured on a high impedance ammeter. The scan is reversed after either the vertex potential (E_v, see Fig. 1) is reached or the current density has reached a value approximately two decades greater than the current density measured at the breakdown potential or critical pitting potential (E_b). The data is plotted with the current density in mA/cm^2 on the x axis (logarithmic axis) versus the potential in mV on the y axis (linear axis).

A GAMRY® potentiostat (G-750) was employed with a scan rate of 1 mV/s over a potential range of −0.1 to 3.0 V_{SCE}. The PBS solutions with and without amino acids were purged with ultra-high purity nitrogen for 30 min prior to immersion of the sample, as well as continuously during the corrosion test. An ICP-MS (Perkin Elmer Sciex, model ELAN DRC-II) was used to determine the concentration of dissolved metal ions in solution after each corrosion test. Five corrosion tests were conducted with each alloy and the average concentrations of metal ions in three replicates of each were determined by ICP-MS. The surface morphology of the alloys was studied before and after corrosion by SEM (JEOL JSM 6330F). A Zhongguo HXD-100 TMC Shanghai Taiming Optical Instruments micro-hardness tester was used to determine the Vicker's hardness, from which an approximation of the tensile strength of each alloys was determined (Ref 8).

2.3 Cell Growth

Human osteoblast cells (hFOB 1.19 cells, ATCC, Manassas, VA, USA) at a concentration of 40,000 cells/mL, were cultivated on the pre-cleaned surface of both alloys in an incubator at 37 °C under 5% CO_2 for 48 h. The cells were then washed with PBS and fixed with 25% formalin solution (1:3 formalin and PBS, Thermo-Shandon, 990244) for SEM analysis (Ref 9).

3. Results and Discussion

The corrosion resistance exhibited by PM and ARC Ti-30Ta alloys revealed that the manufacturing process had a direct effect on the values obtained. For example, the PM alloy exhibited a cyclic polarization curve, which had an anti-clockwise loop at high potential (reverse scan). In this case, the resistance to

Table 1 Average corrosion parameters for Ti-30Ta, PM

Cyclic potentiodynamic polarization measurements			
Corrosion parameters	**PBS**	**PBS-BSA**	**PBS-G-H-T**
E_v, V	2.616	2.360	2.392
E_r, V	−0.174	−0.431	−0.405

corrosion is evaluated by the magnitude of E_v as depicted in Fig. 1. The E_v is determined by noting the maximum potential on the y axis at which the curve loops in an anticlockwise direction during the reverse scan. It should be noted that E_v is reported instead of E_b, if no hysteresis loop is formed (Ref 7). The potentiodynamic scan starts at E_r and scans in the positive direction. The scan direction is reversed after either the E_v is reached or the current density has reached a value approximately two decades greater than the current density measured at the E_b (Ref 7). The reverse scan stops after the current has become less than that in the forward direction or the rest potential is reached, E_r (Ref 7). In the case of Ti-Ta, PM it was observed that E_r and E_v decreased with the addition of amino acids. This may be attributed to the interaction between the amino acids and the surface of the alloys, which resulted in reduced corrosion resistance of the alloy. It has been reported that proteins interact with the repassivation process at the surface of Ti alloys, which influences the resulting surface properties (Ref 10).

Table 1 summarizes the average corrosion parameters E_r and E_v for the Ti-30Ta (PM). This type of cyclic polarization behavior, where the curve loops in an anti-clockwise direction has also been observed with Ni-Ti-Cr (Ref 6). Such alloys are known to resist localized corrosion due to the formation of a mixture of passivating oxides that act as a barrier to metal dissolution. Other researchers (Ref 11-13) have reported similar corrosion behavior with alloys such as Ti-Mo and Ti-Ta, which consist of highly passivating elements. The metal ions released from these alloys are not necessarily related to their elemental composition but is more dependent on the compactness, stability, thickness, and regenerative potential of the oxide film (Ref 4). From a thermodynamic perspective, oxide formation on the surface of Ti-Ta is driven by the Gibbs Free Energy (ΔG) of formation of the following oxides in kcal/mol: TiO_2 (−211), α-TiO (−122), β-TiO (−117), TaO_2 (−50.3), Ta_2O_5 (−456), etc. (Ref 14). Thus, Ta_2O_5 and TiO_2 are highly favored to be produced on the surface of the alloy.

The alloys prepared by ARC melting exhibited cyclic polarization curves with a clockwise loop, i.e., a positive hysteresis. In this case, the resistance to pitting corrosion is evaluated by the difference between the breakdown and the rest potentials ($E_b - E_r$) as shown in Fig. 2. A large hysteresis loop area is usually associated with a greater potential for disruption of the alloy's passive film and lower restoration in surface passivity, which lead to a greater risk of localized corrosion (Ref 15). The hysteresis loop formed by each polarization scan is an indication of the susceptibility to pitting corrosion. Thus, the best performing materials in terms of resistance to pitting corrosion have relatively little or no hysteresis (Ref 15).

Table 2 summarizes the average corrosion parameters E_b, E_r, and $E_b - E_r$, for Ti-30Ta (ARC). The values of E_r and $E_b - E_r$ decreased with the addition of amino acids. Again, this was attributed to the interaction between amino acids and the surface of the alloys. This type of cyclic polarization behavior where the curve loops in a clockwise direction has also been

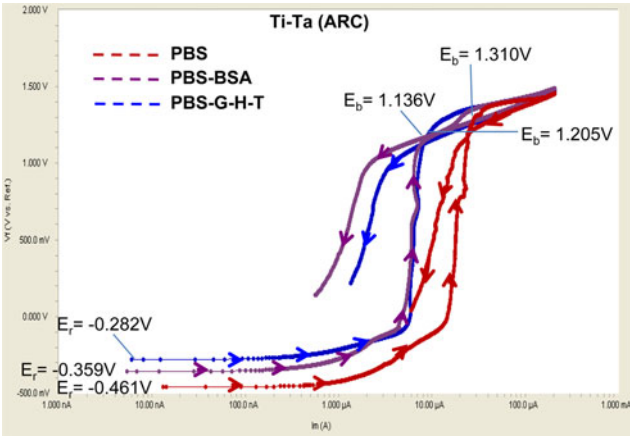

Fig. 2 Cyclic polarization curves for Ti-30Ta (ARC) alloy (clockwise, hysteresis loop) in PBS, PBS-BSA and PBS-G-H-T

Table 2 Average corrosion parameters for Ti-30Ta, ARC

Cyclic potentiodynamic polarization measurements			
Corrosion Parameters	**PBS**	**PBS-BSA**	**PBS-G-H-T**
E_b, V	1.310	1.136	1.205
E_r, V	−0.461	−0.359	−0.282
$E_b - E_r$, V	1.771	1.495	1.487

observed with Ni-Ti and Ni-Ti-Cu (Ref 6). The pH attained before and after corrosion for both alloys in PBS and PBS-amino acids was ≈7.34.

According to Pound (Ref 16), the susceptibility of Nitinol to pitting corrosion can be influenced by the presence and type of amino acids. The metal ions released from metallic materials implanted into the human body are influenced by their composition as well as the environment into which they are placed. Amino acids are essential building blocks in an immense array of macromolecules present in most organisms including blood; the general structure is R–CH(NH_2)–COOH (Ref 17). Amino acids have a zwitterionic or ampholyte character, which are important for the adsorption process. Most amino acids at physiological pH are zwitterionic. Their general properties are characterized by the amino group ($pK \approx 9$), which is positively charged, NH^{+3} at pH < 9 and the carboxylic group ($pK \approx 2$), which is negatively charged, COO^- at pH > 2 (Ref 17). Schmidt and Steinemann (Ref 17) reported that amino acids are readily adsorbed onto the surface of TiO_2 via their carboxyl groups by replacing the basic hydroxyl group on a Ti site. This result in the degradation of the passivating oxidic layer and as observed by the decrease in the value of E_v from 2.6 to 2.4 V for Ti-30Ta PM alloy and the decrease in $E_b - E_r$ value from 1.8 to 1.5 V for Ti-Ta ARC, see Table 1 and 2. The reaction may be described as follows (Ref 17):

$$Ti^+ -^- OH + COO^- + H^+ = Ti^+ -^{--} OOC + H_2O$$

This adsorption mechanism necessitates a specific orientation of the molecule on the surface with the R group oriented further away from the substrate than either the carboxylic or amino group (Ref 17). Schweitzer (Ref 18) reported that Ta is immune to attack by almost all acids under normal conditions. This behavior was confirmed, as no Ta was detected in the solution collected after the corrosion tests.

Table 3 ICP-MS analysis in ppb (μg/L)

	Ti-30Ta (PM)			Ti-30Ta (ARC)		
Analyte	**PBS**	**PBS-BSA**	**PBS-G-H-T**	**PBS**	**PBS-BSA**	**PBS-G-H-T**
Ti	ND	ND	ND	1.43	ND	ND
Ta	ND	ND	ND	ND	ND	ND

Table 3 shows the ICP-MS analysis of dissolved ions in the solution obtained after each corrosion test. The concentration of Ti and Ta ions in solution after corrosion of PM alloy was non-detectable, whereas the solution derived from the corrosion test of the ARC melted alloy contained 1.43 ppb Ti. The presence of Ti in the PBS derived from the Ti-30Ta ARC corrosion test correlated with the size of the hysteresis loop obtained for the cyclic potentiodynamic curve of that alloy in PBS as shown in Fig. 2. As previously discussed, the loop formation is indicative of the alloy's susceptibility to pitting corrosion.

The SEM photomicrographs shown in Fig. 3(a) and (b) revealed a highly pitted surface after corrosion as compared with that obtained prior to corrosion (inset). This may be attributed to the heterogeneous reactive sites on the surface of the alloy that were generated during mechanical polishing, at which pitting corrosion is initiated. In general, the surface of both PM and ARC Ti-30Ta alloys displayed evidence of pitting corrosion (as shown in Fig. 3). However, the latter alloy appeared to be more prone to pitting corrosion. This observation is consistent with the results of other researchers (Ref 4, 10), where alloys manufactured by PM have been reported to have improved resistance to corrosion as compared with their counterparts manufactured by other processes. Alloys manufactured by ARC melting usually develop grain boundaries and dislocations, which serve as initiation sites for pitting corrosion.

The density of both alloys was assessed by Archimedes principle (Ref 19). Ti-30Ta, ARC, and PM alloys exhibited the same density of 5.4 g/cm^3, whereas the theoretical density for both alloys was 5.8 g/cm^3.

Vicker's hardness tests were performed to assess whether the two manufacturing methods had any effect on the alloys mechanical properties. The Vicker's hardness obtained for the ARC melted alloy was 376 and that of the PM alloy was 340. The estimated tensile strengths were 862 and 779 MPa respectively. It should be noted that tensile values are comparable with those of Ni-Ti (Martensitic) (103-1100 MPa) and Ti-Ta alloys (587-1000 MPa) (Ref 8, 20, 21).

Human osteoblast cells were successfully cultivated on the surface of both alloys as shown in Fig. 4. The viability exhibited by the cells was indicative of the materials biocompatibility. However, no discernable difference in osseointegration was observed with either alloy after a 48 h growth period. Therefore, further tests need to be conducted over a longer growth period to determine whether the manufacturing process has any affect on osseointegration.

4. Conclusions

This investigation revealed that the resistance to pitting corrosion of Ti-30Ta is influenced by its manufacturing process. The cyclic potentiodynamic corrosion curve for Ti-Ta, PM displayed an anti clockwise loop, whereas the ARC melted alloy displayed a clockwise loop with hysteresis. The alloy

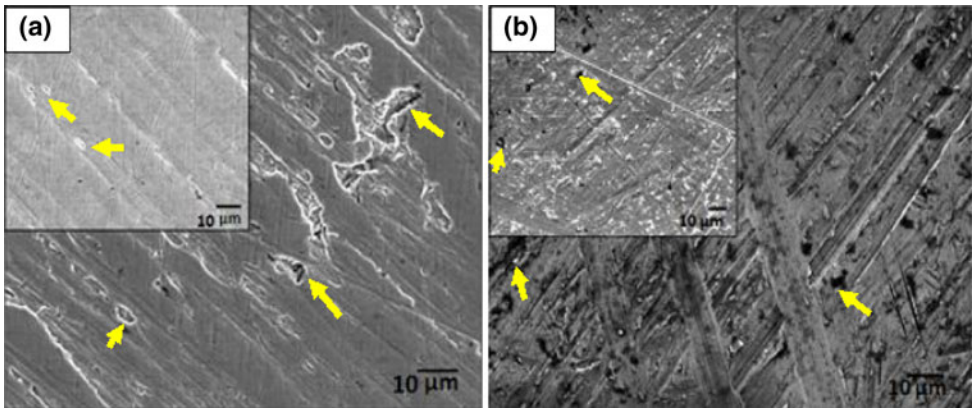

Fig. 3 Surface morphology of Ti-Ta alloys before (inset) and after corrosion: (a) Ti-Ta PM and (b) Ti-Ta ARC

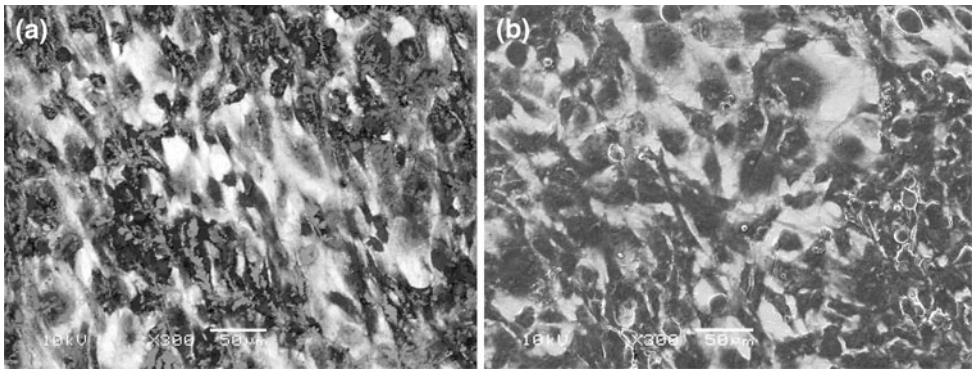

Fig. 4 Osteoblast cell growth: (a) Ti-Ta (PM) and (b) Ti-Ta (ARC)

manufactured by PM was more resistant to localized corrosion as compared with that manufactured by ARC melting. Both alloys revealed a moderately pitted surface after corrosion with little or no metallic dissolution. However, the corrosion susceptibility of Ti-30Ta alloys appeared to increase with the addition of amino acids to PBS. The growth of human osteoblast cells on both the alloys, as well as their good corrosion resistance and mechanical properties suggest that Ti-30Ta is a very promising biomaterial.

Acknowledgments

The project described was supported by Award Number SC3GM084816 from the National Institute of General Medical Sciences. The author would like to acknowledge Dynamet Technology Inc., Burlington, MA, USA for supplying the Ti-30Ta PM alloy, Frank Biancaniello and NIST for manufacturing the ARC melted Ti-30Ta alloy and Dr. Vekalet Tek for her assistance in preparation of amino acids.

References

1. M. Niinomi, Recent Research and Development in Titanium Alloys for Biomedical Applications and Healthcare Goods, *Sci. Technol. Adv. Mater.*, 2003, **4**, p 445–454
2. Joining Joints, Austin Weber, Asssemblymag.com, December 22, 2008
3. H. Suh, Recent Advances in Biomaterials, *Yonsei Med. J.*, 1998, **39**(2), p 87–96
4. P.K.S. Gill, N. Munroe, C. Pulletikurthi, S. Pandya, V. Tek, and W. Haider, In-Vitro Localized Corrosion Studies of Ti-Ta Alloy, Extended Abstract—SMST, Pacific Grove, California, May 16-20, Vol 25761, 2010, p 120–121
5. N.T.C. Oliveira and A.C. Guastald, Electrochemical Stability and Corrosion Resistance of Ti–Mo Alloys for Biomedical Applications, *Acta Biomater.*, 2009, **5**, p 399–405
6. H. Waseem, "Enhanced Biocompatibility of NiTi (Nitinol) Via Surface Treatment and Alloying," FIU Electronic Theses and Dissertations, 2010, Paper 177
7. "Standard Test Method for Conducting Cyclic Potentiodynamic Polarization Measurements to Determine the Corrosion Susceptibility of Small Implant Devices," ASTM F 2129-08, Annual Book of ASTM Standards
8. E.A. Trillo, C. Ortiz, P. Dickerson, R. Villa, S.W. Stafford, and L.E. Murr, Evaluation of Mechanical and Corrosion Biocompatibility of TiTa Alloys, *J. Mater. Sci. Mater. Med.*, 2001, **12**, p 283–292
9. J.E. Tercero, S. Namin, D. Lahiri, K. Balani, N. Tsoukias, and A. Agarwal, Effect of Carbon Nanotube and Aluminum Oxide Addition on Plasma-Sprayed Hydroxyapatite Coating's Mechanical Properties and Biocompatibility, *Mater. Sci. Eng.*, 2009, **C 29**, p 2195–2202
10. W. Haider, N. Munroe, P. Gill, and C. Pulletikurthi, The Electrochemical Characteristics of Surface Treated Nitinol Alloys, NACE International, Corrosion, March 14–18, 2010, San Antonio, TX
11. Y.L. Zhoua, M. Niinomi, T. Akahori, H. Fukui, and H. Toda, Corrosion Resistance and Biocompatibility of Ti–Ta Alloys for Biomedical Applications, *Mater. Sci. Eng. A*, 2005, **398**, p 28–36
12. M.A. Khan, R.L. Williams, and D.F. Williams, The Corrosion Behavior of Ti-6Al-4, Ti-6Al-7Nb and Ti-13Nb-13Zr in Protein Solutions, *Biomaterials*, 1999, **20**, p 631–637
13. R. Bhola, S.M. Bhola, B. Mishra, and D.L. Olson, Electrochemical Behavior of Titanium and Its Alloys as Dental Implants in Normal Saline, *Res. Lett. Phys. Chem.*, Article ID 574359, 2009, p 1-4

14. JANAF Thermodynamical Tables, Second Edition, Issued June 1971
15. http://www.andersonmaterials.com/electro_case_study_2.html, accessed, June 2, 2010
16. B.G. Pound, Corrosion Behavior of Nitinol in Blood Serum and PBS Containing Amino Acids, *J. Biomed. Mater. Res. B*, 2010, **94**(2), p 287–295
17. M. Schmidt and S.G. Steinemann, XPS Studies of Amino Acids Adsorbed on Titanium Dioxide Surfaces, *Fresenius' J. Anal. Chem.*, 1991, **341**, p 412–415
18. P.A. Schweitzer, *Fundamentals of Metallic Corrosion: Atmospheric and Media Corrosion of Metals (Corrosion Engineering)*, CRC Press, 2007, p 542–543
19. R.W. Grimshaw, The Chemistry and Physics of Clays and Other Ceramic Materials, Ernst Benn Ltd., London, 1971, p 417–422, 441–442
20. Y.L. Zhou, M. Niinomi, and T. Akahori, Effects of Ta Content on Young's Modulus and Tensile Properties of Binary Ti–Ta Alloys for Biomedical Applications, *Mater. Sci. Eng. A*, 2004, **371**, p 283–290
21. J. Ryhänen, Biocompatibility Evaluation of Nickel-Titanium Shape Memory Metal Alloy, Department of Surgery, Oulu, 1999, 29